

Article

Quantitative Identification of Water Sources of Coalbed Methane Wells, Based on the Hydrogen and Oxygen Isotopes of Produced Water—A Case of the Zhijin Block, South China

Lingling Lu ^{1,*}, Chen Guo ^{2,3} , Zhenlong Chen ⁴ and Hang Yuan ⁴

¹ Aerial Photogrammetry and Remote Sensing Bureau of China Administration of Coal Geology, Xi'an 710199, China

² College of Geology and Environment, Xi'an University of Science and Technology, Xi'an 710054, China

³ Shaanxi Provincial Key Laboratory of Geological Support for Coal Green Exploitation, Xi'an 710054, China

⁴ East China Oil & Gas Company, Sinopec, Nanjing 210011, China

* Correspondence: lu_lingling13@126.com; Tel.: +86-15991666428

Abstract: The quantitative identification of water sources is an important prerequisite for objectively evaluating the degree of aquifer interference and predicting the production potential of coalbed methane (CBM) wells. However, this issue has not been solved yet, and water sources are far from being completely understood. Stable water isotopes are important carriers of water source information, which can be used to identify the water sources for CBM wells. Taking the Zhijin block in the Western Guizhou Province as an example, the produced water samples were collected from CBM wells. The relationships between the stable isotopic compositions of the produced water samples and the production data were quantitatively analyzed. The following main conclusions were obtained. (1) The δD and $\delta^{18}O$ values of the produced water samples were between -73.37‰ and -27.56‰ (average -56.30‰) and between -11.04‰ and -5.93‰ (average -9.23‰), respectively. The water samples have D-drift characteristics, showing the dual properties of atmospheric precipitation genesis and water–rock interaction modification of the produced water. An index d was constructed to enable the quantitative characterization of the degree of D-drift of the produced water. (2) The stable isotopic compositions of produced water showed the control of the water sources on the CBM productivity. The probability of being susceptible to aquifer interference increased with the increasing span of the producing seam combination, reflected in the lowering δD and $\delta^{18}O$ values and the decreasing gas productivity. (3) Three types of water, namely, static water, dynamic water, and mixed water, were identified. The characteristic values of the isotopic compositions of the static and dynamic water were determined. Accordingly, a quantitative identification method for the produced water sources was constructed, based on their stable isotopic compositions. The identification results have a clear correlation with the gas production, and the output of the static water contributes to the efficient CBM production. The method for the quantitative identification of the water sources proposed in this study, can help to improve the CBM development efficiency and optimize the drainage technology.

Keywords: coalbed methane co-production; produced water sources; stable isotopes; interlayer interference; dynamic water; static water; Western Guizhou



Citation: Lu, L.; Guo, C.; Chen, Z.; Yuan, H. Quantitative Identification of Water Sources of Coalbed Methane Wells, Based on the Hydrogen and Oxygen Isotopes of Produced Water—A Case of the Zhijin Block, South China. *Energies* **2022**, *15*, 9550. <https://doi.org/10.3390/en15249550>

Academic Editor: Dameng Liu

Received: 5 November 2022

Accepted: 13 December 2022

Published: 16 December 2022

Publisher's Note: MDPI stays neutral with regard to jurisdictional claims in published maps and institutional affiliations.



Copyright: © 2022 by the authors. Licensee MDPI, Basel, Switzerland. This article is an open access article distributed under the terms and conditions of the Creative Commons Attribution (CC BY) license (<https://creativecommons.org/licenses/by/4.0/>).

1. Introduction

Efficient coalbed methane (CBM) development technologies are crucial for increasing the domestic oil and gas supply capacity in China, easing the contradiction between the supply and demand of oil and gas and achieving a clean and sustainable development of energy from fossil fuels [1–3]. CBM resources are found in coal seams deposited in coal-bearing basins, and the implementation of a multi-seam CBM coproduction is a necessary method for improving the CBM development efficiency [4–6]. However, the interlayer differences in the geological conditions and the reservoir characteristics have caused serious

interference problems during the CBM multi-seam coproduction, limiting the CBM production and even causing the failure of CBM development projects [7–16]. CBM development is a gas–water two-phase flow process, and the interlayer interference has a direct reflection in the quantity and quality characteristics of the gas and water production [17,18]. The geochemical composition of the produced water of the CBM wells contains rich information on the produced water sources and can be used for evaluating the CBM production potential and discriminating the interference degree for the multi-seam CBM coproduction [7,19–24]. The CBM coproduction from multiple coal seams is susceptible to communicating with different hydrogeological units or hydrodynamic systems, affording complex and variable produced water sources, and the differences in the produced water sources directly affect the reservoir pressure reduction efficiency and the gas production capacity [8,25–29]. The effective identification of the water sources for the CBM coproduction wells is the basis for analyzing the interlayer interference of the coproduction wells and implementing the subsequent adjustments of the development plan.

Stable hydrogen/oxygen isotopes are one of the many geochemical properties of produced water and carry information about the origin of the groundwater and its evolution and movement. Further, they are relatively weakly influenced by engineering factors, which can provide an important basis for identifying the sources of produced water [30–34]. Previous studies have investigated the hydrogen and oxygen isotopic compositions of produced water from the CBM wells, by describing their formation mechanisms and evolution processes, analyzing the main controlling factors from both geological and engineering perspectives, and forming a preliminary principle and method to identify the produced water sources, and the interference degree, based on the hydrogen and oxygen isotopes [7,35–37]. However, the qualitative studies have been mostly the focus and there has been no quantitative investigation on the produced water sources, leading to the insufficient guidance for the CBM development.

Western Guizhou is in the active phase of the CBM development, with well-developed multiple and thin coal seams in the Upper Permian coal-bearing strata. The research object herein is the Upper Permian coal-bearing strata in the Zhijin block of Western Guizhou, South China. The analysis of the hydrogen and oxygen isotopic compositions of the produced water from the CBM coproduction wells was conducted, and their intrinsic relationship with the CBM production capacity was revealed. On this basis, the studies on the implications of the isotopic compositions of the produced water for the water source discrimination were conducted, and the quantitative stable isotope analysis of the produced water sources was offered. This study aimed to enrich the geological theory and methods of the CBM coproduction, especially the method for quantitatively discriminating water sources, based on the geochemical characteristics of produced water, and to provide a reference for achieving the economic and efficient CBM coproduction in multi-seam areas.

2. Geological Setting

The Zhijin block, Western Guizhou is an important CBM block in South China with a geological resource of 461.851 billion m³ of CBM, at a burial depth of less than 1000 m and a resource abundance of 128 million m³/km² [38]. This block is rich in CBM resources with a moderate burial depth and relatively intact coal body structure, which shows great promise for the CBM development [11]. Tectonically, the Zhijin block belongs to the Qianzhong uplift of the Yangzi plate, South China and contains the gas-producing Yanjiao syncline, with a coal-bearing area of about 1000 km², along with the Qianxi syncline. The Yanjiao syncline is a compound syncline, mainly containing the coal-bearing Bide, Shuigonghe, Santang, Agong, and Zhucang sub-synclines [39]. The tectonic orientation of the Yanjiao syncline is mainly in the NW- and NE-trending, formed under the NE–SW and NW–SE maximum principal stress in the middle and late Yanshanian period, respectively. The NW-trending structures experienced a more complex tectonic transformation, causing more adverse geological conditions for the CBM development, than those of the NE-trending structures [12] (Figure 1). The coal and CBM resources are mainly located in the sub-

synclines, among which the best conditions for the CBM development are in the Zhucang sub-syncline, characterized with a high gas content (>15 m³/t), moderate burial depth, relatively intact coal body structure, and a high permeability [9]. It is also the main area for the CBM exploration and development at present in the Zhijin block.

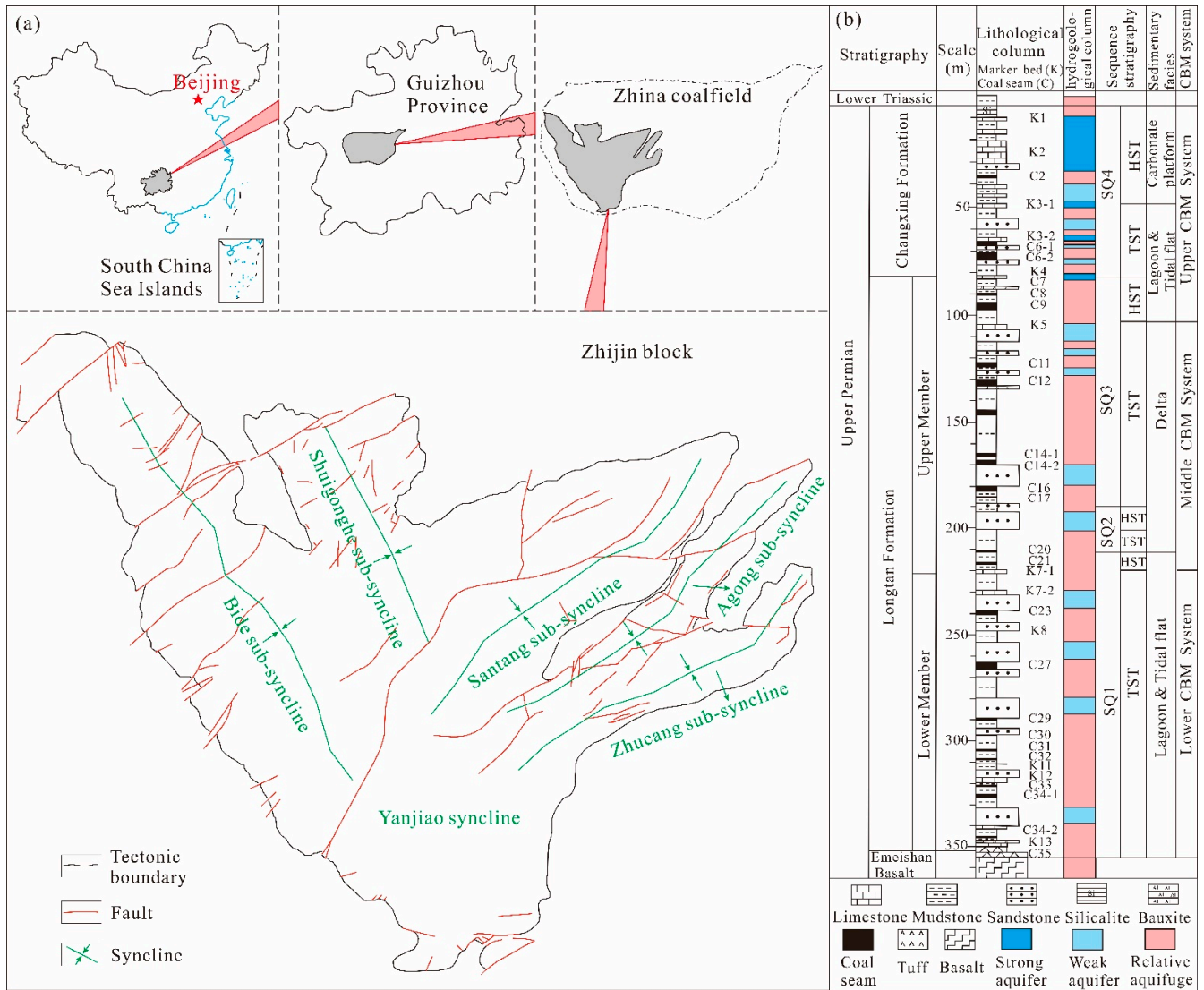


Figure 1. Geological setting of the Zhijin block, Western Guizhou. (a) Tectonic map. (b) Stratigraphic column.

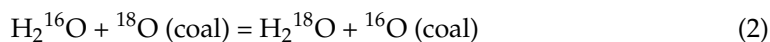
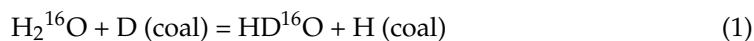
The main coal-bearing strata in this area are the Upper Permian Longtan Formation, deposited in a tidal lagoon flat delta sedimentary system, and the Changxing Formation, formed in a carbonate tidal flat carbonate platform environment [9]. The Upper Permian coal-bearing strata are in pseudoconformity contact with the overlying Lower Triassic Feixianguan Formation and with the underlying Emeishan Basalt Formation [40,41].

3. Principles and Methods

3.1. Principles of the Groundwater Stable Isotopic Analysis

The stable isotopic composition of the groundwater can indicate the groundwater origin, evolution, and age [33]. Generally, shallow groundwater has a relatively light isotopic composition, and the isotopic exchange reaction between the groundwater and rocks (including coal seams) during the groundwater flow toward the deep, tends to increase the heavy isotope proportion [7]. The isotopic exchange reaction can be seen

as a part of water/rock interactions. The heavy isotopes ^{18}O and D are easily enriched in the closed and stagnant groundwater, which is one of the basic principles of isotopic hydrogeochemistry. The isotope exchange reactions involved in the coal-bearing strata include the following.



In a closed groundwater environment, the above reactions are long-lasting and gradually intensify, leading to the increasingly heavier stable isotopes in the groundwater with enhanced water/rock interactions. Hence, stable isotope composition can be used as an important indicator to discriminate the dynamic conditions of the groundwater. A heavier hydrogen and oxygen isotopic composition (higher δD and $\delta^{18}\text{O}$) reflects a higher degree of the groundwater retention and a poorer recharge and flowability conditions. This can provide a basis for identifying the sources of water produced from the CBM wells and then determining the effect of the water production on the pressure reduction, as well as the gas desorption and production in the reservoirs. Moreover, the isotopic composition of the surface water can be heavier, due to the evaporative fractionation effect, which is particularly evident in arid and semiarid regions [42].

3.2. Classification of the Water Sources for the CBM Wells

The CBM development relies on water production and reservoir pressure reduction, and the difference of the produced water source controls the pressure reduction and gas production efficiency. The produced water in the CBM wells can generally be divided into internal and external sources [43], which basically corresponds to the concept of “static water storage” and “dynamic water storage”, in hydrogeology [44–46]. When the drainage is recharged by a cross-flow from the aquifers or surface water outside the producing coal seam, that results in an abnormal increase in the water production but a low efficiency of the pressure reduction and gas production, it is called the external source water or dynamic water. When the drainage does not communicate with the strong aquifers, the produced water comes from the limited water storage within the producing coal seam and its adjacent roof and floor, which can effectively promote the reservoir pressure reduction and gas desorption; this is called the internal source water or static water. In terms of the effectiveness of the drainage for the gas production of the CBM well, the internal source water is “effective” water and the external source water is “ineffective” water. Many CBM engineering practices reveal the external source water to be the main cause of the high water production and low gas production. The identification of the produced water sources is important to evaluate the CBM well drainage efficiency and to discriminate the interlayer interference during the CBM coproduction in multiple coal seams.

3.3. Sample Collection and Tests

Twelve produced water samples were collected from the water outlets of 12 CBM wells in the Zhijin block in October 2021, involving vertical, directional, and horizontal wells, by washing a sampling polyethylene bottle with the target water three times before collection and ensuring that the water sample was filled and sealed in the sampling bottle. Except for the single-seam production horizontal wells, the rest are multi-seam coproduction wells. Table 1 lists the production information of each well. In addition, one surface water sample was collected from the Shaopu River flowing through the Zhijin block with the above sampling method. The water samples were tested on site during the sample collection for the water temperature, pH, total dissolved solids (TDSs), and electrical conductivity. The hydrogen and oxygen stable isotope testing was performed using a MAT-253 stable isotope mass spectrometer (Thermo Electron, Finnigan, Inc., San Jose, CA, USA) at the State Key Laboratory of Environmental Geochemistry, Institute of Geochemistry, Chinese Academy of Sciences (Guiyang) at the ambient temperature and pressure in a light-free environment.

The measured results were reported in delta notation (δ) in per mil (‰) relative to the known standards (VSMOW, Vienna Standard Mean Ocean Water), with analytical precision values of less than $\pm 1\text{‰}$ and less than $\pm 0.2\text{‰}$ for δD and $\delta^{18}O$, respectively [7]. Each water sample underwent duplicate testing to guarantee the precision and accuracy of the analyses. The outcomes were essentially identical and could satisfy quality control standards. Figure 2 illustrates the geometric characteristics of the production coal seams in Table 1.

Table 1. Information on the CBM wells.

Well Number	Well Type	Fracturing and Production Coal Seams	Geometric Characteristics of the Production Coal Seams (m)			Average Daily Production (m ³ /d)		Peak Daily Gas Production (m ³ /d)
			Burial Depth	Maximum Span	Total Producing Thickness	Water	Gas	
1	Vertical	20/23, 6/7/8/10, 12/14/16/17	240.4–432.3	191.9	5.0	1.04	118	146
2	Horizontal	23 (8)	585.3–587.4	2.1	2.1	4.24	2660	3066
3	Vertical	23/30, 32/33/34	477.2–546.1	68.9	2.1	16.53	0	0
4	Vertical	23/24/27, 30/32/33	1093.4–1155.0	61.6	5.4	1.58	1022	2382
5	Vertical	14, 16	562.0–615.7	53.7	3.9	5.45	358	1107
6	Vertical	20/21/23, 27/30	517.5–598.1	80.6	5.1	1.45	1058	1209
7	Vertical	19/20, 23/27	509.8–557.6	47.8	5.2	0.73	1302	1529
8	Vertical	20/21/23, 27/30	806.3–899.3	93.0	6.7	6.82	17	147
9	Directional	16/17, 20/23, 27/30	415.0–663.8	248.8	9.9	1.20	1324	1455
10	Horizontal	23 (7)	539.3–542.1	2.8	2.8	0	2118	2215
11	Horizontal	30 (9)	602.4–604.8	2.4	2.4	0	2219	2438
12	Directional	11/12/13, 16/17/18/19, 20/21/23, 27/30	453.3–642.0	188.7	9.9	0	2662	3140

Notes: In the column of the fracturing and production coal seams, the number represents the coal seam number, which can be found in the lithological column of Figure 1, the separation “,” represents the different fracturing sections, “/” represents the same fracturing section, and the number in parentheses represents the number of fracturing sections of the horizontal well. The data format in the burial depth column is the “burial depth of the top boundary- burial depth of the bottom boundary”.

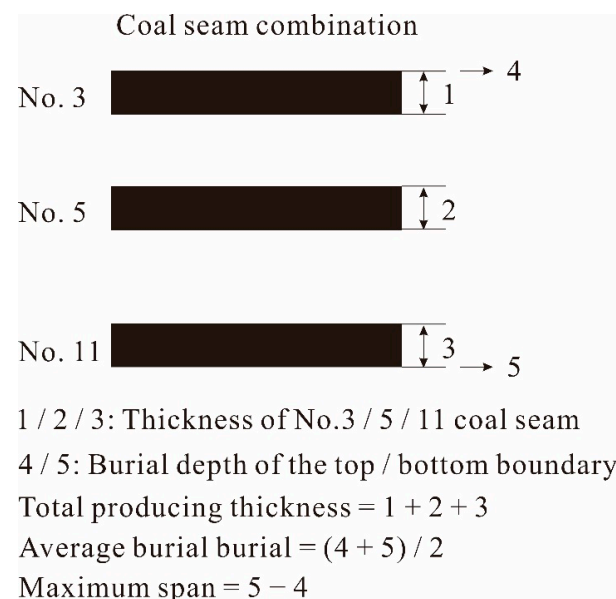


Figure 2. Illustration of the geometric parameters of the production coal seams.

4. Results and Discussion

4.1. Stable Isotopic Compositions

The test results show that the δD of the water samples ranged from -73.37‰ to -27.56‰ , with an average of -56.30‰ , and $\delta^{18}O$ ranged from -11.04‰ to -5.93‰ , with an average of -9.23‰ (Table 2). According to the local meteoric water line (LMWL) in Southwest China, the water samples are distributed along the LMWL and are located at the upper left of the LMWL (Figure 3). The production coal seams of the CBM wells are generally shallower than 800 m, resulting in a certain degree of similarity between the isotopic composition of the produced water and that of the surface water or atmospheric precipitation. However, compared with surface water sample No. 13, the produced water of the CBM wells generally has a heavier hydrogen/oxygen isotopic composition and a more significant D-drift trend, reflecting the further modification effect of the groundwater circulation and the water/rock interaction on the produced water. The D-drift trend indicated a heavier δD of the sample than the LMWL, based on a same $\delta^{18}O$, characterized by the data falling on the upper left of the LMWL.

Table 2. Test results of the stable hydrogen/oxygen isotope and the water quality parameters of the water samples.

Well Number	Sample Number	δD (‰)	Standard Deviation (‰)	$\delta^{18}O$ (‰)	Standard Deviation (‰)	<i>d</i>	pH	EC ($\mu S/cm$)	TDS (mg/L)
1	1	-73.37	0.58	-11.04	0.19	5.01	7.78	1963	949
2	2	-36.33	0.55	-7.14	0.07	11.02	7.47	9890	4523
3	3	-71.05	0.55	-10.77	0.08	5.13	8.37	1988	944
4	4	-54.88	0.08	-9.32	0.24	9.76	7.61	5470	2681
5	5	-71.11	0.35	-10.85	0.09	5.71	7.52	2080	1123
6	6	-65.05	0.16	-10.16	0.06	6.31	7.94	2920	1562
7	7	-53.52	0.40	-9.13	0.02	9.67	7.75	4310	2152
8	8	-61.41	0.45	-9.98	0.03	8.51	7.99	2950	1568
9	9	-58.99	0.48	-9.79	0.09	9.42	7.98	3170	1678
10	10	-27.56	0.45	-5.93	0.07	10.11	7.62	15,540	8800
11	11	-44.16	0.57	-7.07	0.06	2.58	8.44	7590	3603
12	12	-58.15	0.54	-9.53	0.03	8.16	8.43	4410	2240
River	13	-67.94	0.20	-9.90	0.07	1.32	8.2	332	166

Notes: The sample numbers correspond to the CBM well numbers, for example, sample No. 1 was collected from well No. 1. Sample No. 13 was from the Shaopu River. *d* is the D drift index, as described below.

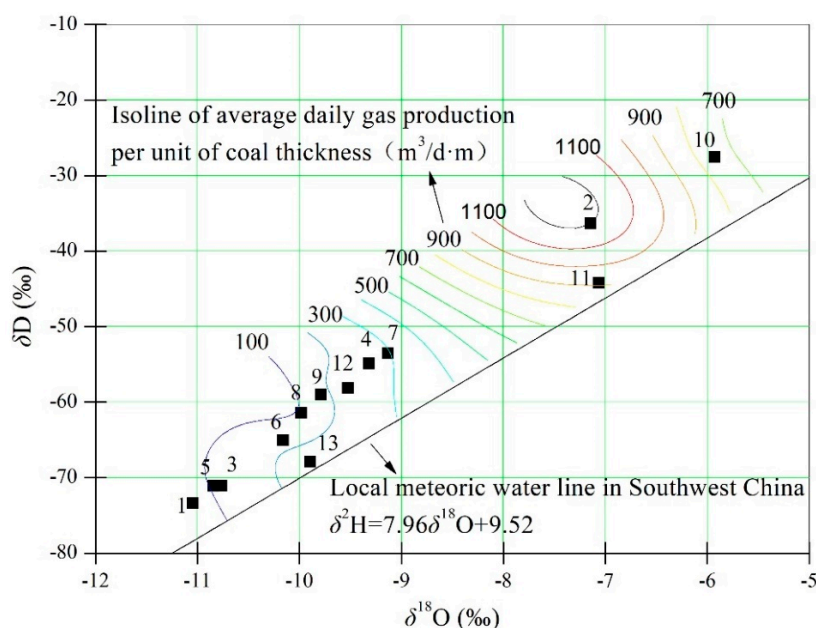


Figure 3. Relationship between the $\delta^{18}O$ and δD values of the water samples.

Surface water sample No. 13 is very close to the LMWL and has a lighter isotopic composition, compared to majority of the produced water samples. The stable isotopes of the surface water tend to be heavier in areas with strong evaporation in arid climates due to the evaporative fractionation effect [7]. The climate in the study area is relatively humid, but the evaporative fractionation should still be the main reason of the heavier isotopic composition of the surface water sample, than some produced water samples (samples 1, 3, and 5). Sample 11 is also close to the LMWL but has a heavy isotopic composition, indicating strong water/rock interactions. The rest of the samples showed obvious D-drift characteristics (Figure 3). The causes of the D-drift trend in the produced water of the CBM wells can be explained as follows [7,37]: (1) Coal contains various hydrogen-containing compounds, and the number of hydrogen atoms exceeds the number of oxygen atoms. The coal-bearing strata are generally in a reducing environment, and the light hydrogen isotopes in water can exchange with heavy hydrogen isotopes in coal in an isotopic exchange reaction. (2) CH₄ can be dissolved in groundwater in large quantities under high-temperature conditions, and when sulfate is present in the groundwater, CH₄ can induce the reduction of sulfate, to produce H₂S, thus causing the isotope exchange in the H₂S–H₂O or CH₄–H₂O system and making the hydrogen isotopes in water heavier. The reaction can be expressed as



In conclusion, the hydrogen isotope exchange reactions are more intense than the oxygen isotope exchange reactions for the coal measure water or the coal seam water, resulting in the CBM produced water with D-drift characteristics. The D-drift is the result of the interaction between the organic composition of the coal seam and the groundwater in a hydrogen-rich geological environment, which can reflect the characteristic of the static water and help depressurize the reservoir after the output. Previous studies also revealed that the higher the degree of the D-drift in the isotopic composition of the produced water, the higher the CBM production [7]. The quantitative characterization of the D-drift index is necessary for predicting the CBM productivity.

To quantitatively characterize the degree of the D-drift trend, the D-drift index, d , defined as the erect distance between the isotopic data point of the water samples in Figure 1 and the LMWL, is calculated using the formula below. The larger the distance, the stronger the D-drift represented.

$$d = \delta\text{D} - 7.96 \times \delta^{18}\text{O} - 9.52 \quad (5)$$

where d is the D-drift index and δD and $\delta^{18}\text{O}$ are the measured data of the samples. The D-drift indexes of the produced water samples are calculated to be 2.58 (No. 11)–11.02 (No. 2) (average 7.62). The lowest D-drift index of 1.32 is measured for sample No. 13, indicating that it responds most strongly to the atmospheric precipitation (Table 2).

4.2. Relationships between the Stable Isotopic Composition and Production

Figure 2 shows the geometric characteristics of the production coal seam combination in Table 1. The production parameters of the CBM wells were further defined as follows. The average daily gas production is the average of all of the daily gas production of the sampling month; the peak daily gas production is the maximum value of the daily gas production of the sampling month; the average daily gas production per unit of coal thickness is the ratio of the average daily gas production and the total producing thickness. Similarly, the calculation methods of the water production parameters were consistent with the above gas production parameters.

The correlations among the hydrogen and oxygen isotopic compositions of the produced water, the geometric parameters of the production seam combination, and the production parameters were analyzed. Among the geometric parameters, the maximum span shows a negative correlation with the isotopic compositions, which can be seen as an

important geometric factor controlling the water production characteristics. This suggests that the smaller the span, the stronger the water/rock (coal) interactions, which is reflected in the heavy stable isotopic compositions and is conducive to the CBM production after the water output (Table 3).

Among the burial depth parameters, the top boundary burial depth correlates best with the isotopic compositions of the produced water, implying that the coproduction interference mainly comes from the upper aquifer (Table 3). In addition, δD has a significant positive correlation with $\delta^{18}O$, reflecting their commonality in the groundwater chemistry formation and similar hydrogeological implications. The test results herein show that δD and $\delta^{18}O$ have a significant positive correlation with the TDSs, which can be used as a reference to identify the hydrodynamic conditions of the produced water (Figure 4).

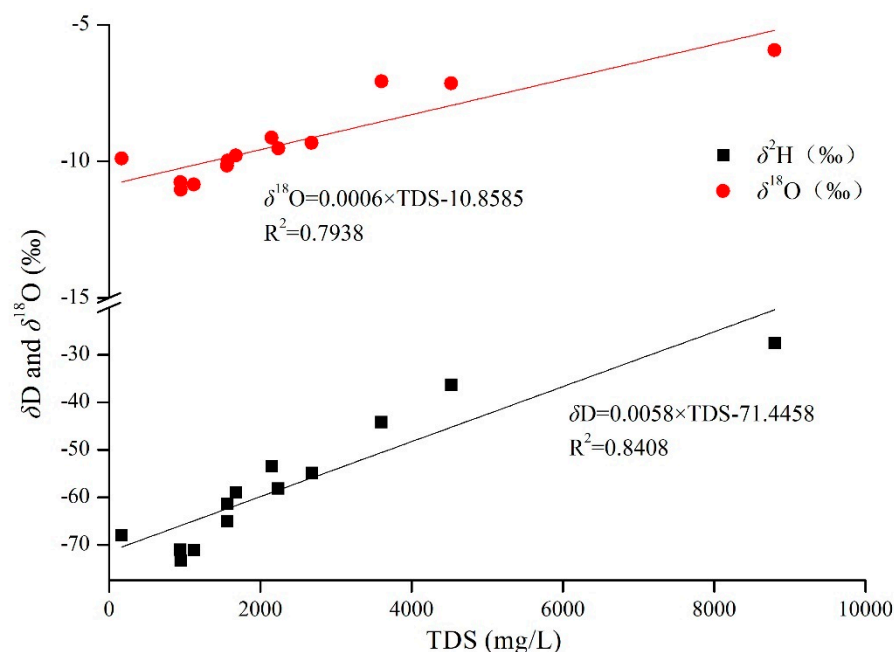


Figure 4. Relationship between the isotopic compositions and the TDSs of water samples.

δD and $\delta^{18}O$ have a good positive correlation with the gas production parameters, providing favorable conditions for predicting the gas production, based on the produced water isotopic compositions. The average daily gas production per unit coal thickness has the best correlation with the isotopic compositions, with a correlation coefficient greater than 0.85. The δD and $\delta^{18}O$ values showed a weak negative correlation with the water production parameters, among which the peak daily water production was relatively well correlated, followed by the average daily water production. The average daily water production per unit coal thickness has the lowest correlation with δD and $\delta^{18}O$.

The average daily gas production per unit coal thickness is a typical indicator to characterize the production capacity of the CBM coproduction wells, which can eliminate the influence of the coal thickness on the gas production. The isotopic compositions of the produced water can effectively reflect the water source types and the reservoir depressurization efficiency, which is directly reflected in the gas production level per unit coal thickness, and thus, the two have a good correlation. Meanwhile, the low correlation between the isotopic compositions of the produced water and the average daily water production per unit coal thickness indicates that the water production of the gas wells is not directly related to the thickness of the producing coal seam but mainly due to the water sources. The larger the span, the easier it is to connect with the different water sources, which is directly reflected in the increase in the peak daily water production and average daily water production. Hence, the peak daily water production and average daily water production have a better correlation with the produced water isotopic compositions.

Table 3. Correlation coefficients between the stable isotopic compositions of the produced water and the production parameters.

Isotopes	Isotopes			Geometric Characteristics of the Production Seam Combination (m)					Daily Gas Production			Daily Water Production		
	D	O	<i>d</i>	Top Boundary Burial Depth	Bottom Boundary Burial Depth	Average Burial Depth	Maximum Span	Total Producing Thickness	Average	Peak	Average Per Unit Coal Thickness	Average	Peak	Average Per Unit Coal Thickness
D	1	0.979 **	0.519	0.223	0.016	0.127	−0.544	−0.293	0.778 **	0.707 *	0.854 **	−0.410	−0.421	−0.308
O	0.979 **	1	0.333	0.180	−0.050	0.072	−0.587 *	−0.371	0.773 **	0.687 *	0.883 **	−0.402	−0.420	−0.290
<i>d</i>	0.519	0.333	1	0.310	0.339	0.330	−0.006	0.274	0.348	0.392	0.204	−0.209	−0.180	−0.223

Notes: ** Significantly correlated at the 0.01 level, * Significantly correlated at the 0.05 level.

Among the geometric parameters of the production seam combination, the maximum span exerts the most important influence on the produced water isotopic compositions. The possibility of recharging from the upper aquifer during the drainage increases as the span increases, characterized by the gradual lightening of the isotopic compositions. The larger the span, the lower the average daily gas production per unit coal thickness, and the higher the peak water production. To reduce the chance of the interlayer interference and to improve the coproduction efficiency, the span of the production layer combination should not be too large and the burial depth should not be too shallow.

To be specific, an average of 7.24 m of the total producing thickness of the CBM wells in the study area is measured; thus, a level of $138 \text{ m}^3/(\text{d}\cdot\text{m})$ of the average daily gas production per unit coal thickness can ensure that the average daily gas production of a single well achieves the industry standard of $1000 \text{ m}^3/\text{d}$. The relationships of the average daily gas production per unit coal thickness with the maximum span and burial depth of the top boundary of the production coal seam combination are illustrated in Figure 5. The level of $138 \text{ m}^3/(\text{d}\cdot\text{m})$ of the average daily gas production per unit coal thickness corresponds to a 67 m maximum span (Figure 5a) and 440 m top boundary burial depth (Figure 5b). Practically, a maximum span of less than 70 m and a top boundary burial depth deeper than 400–450 m should be used when determining the coal seam combinations for the CBM coproduction in the study area. The optimal burial depth of the top boundary for the CBM production is 600–650 m (Figure 5b).

Moreover, the average daily gas production per unit coal thickness shows a positive correlation with d , following the function shown in Figure 6. When the d exceeded 9.42, the gas production increased rapidly and there was a positive correlation; when the d was less than 9.42, the correlation was not significant. It is assumed that the threshold value of d is 9.42 to distinguish the coal seam water from other water sources, beyond which the characteristics of the coal seam water gradually appear and intensify, and the gas production efficiency then increases. An anomalous data point (Sample 11) can be observed in the figure, which has a low d but relatively heavy isotopic compositions, corresponding to a high gas production (Figure 6).

The removal of Sample 11 revealed that all produced water samples show a highly linear relationship, indicating the anomalous nature of Sample 11 (Figure 7). In addition, subtracting the fitted linear equation ($y = 9.05x + 27.89$) in Figure 7 from the LMWL equation ($y = 7.96x + 9.52$) yields an equation reflecting the relationship between the degree of the D-drift and $\delta^{18}\text{O}$:

$$y = 1.09x + 18.37 \quad (6)$$

It can be seen that the degree of the D-drift increases with $\delta^{18}\text{O}$, which also indicates that the more intense the water/rock interaction of the coal seam water (gradual increase of δD and $\delta^{18}\text{O}$), the more obvious the D-drift trend.

4.3. Classification of the Produced Water Sources

Based on the hydrogen/oxygen isotopic compositions (δD and $\delta^{18}\text{O}$) and d of the water samples, the Q-mode hierarchical clustering analysis was conducted to discriminate their relationships. The results showed a classification of all samples into four major groups by a distance measurement of 5 (Figure 8).

- (1) The first group (Cluster 1) includes Samples 1, 3, 5, 6, and 13, containing surface water sample (No. 13) characterized by the light hydrogen and oxygen isotope compositions (Figures 8 and 9). δD and $\delta^{18}\text{O}$ were measured to be -73.37 – -65.05 ‰ (average -69.70 ‰) and -11.04 – -9.90 ‰ (average -10.54 ‰). The d values were between 1.32 and 6.31 (average 4.70). The hydrogen and oxygen isotopic compositions reflect the weak water/rock interaction and the strong mobility of the produced water, suggesting that the drainage is recharged by the external water from the upper aquifers. This group mostly corresponds to the low gas production wells. The average daily gas production per unit coal thickness values are 0 – $207.45 \text{ m}^3/\text{d}\cdot\text{m}$ (average $80.71 \text{ m}^3/\text{d}\cdot\text{m}$); the average daily water production values are 1.04 – $16.53 \text{ m}^3/\text{d}$ (average $6.12 \text{ m}^3/\text{d}$).

The well type is vertical, which is easy to communicate with the aquifers under multi-seam separated or joint fracturing conditions. Sample 1 was from Well 1, and the previous study confirmed the interference of the shallow groundwater in the drainage of this well [7]. Sample 3 was from Well 3, which is located in the Santang sub-syncline, and has been producing only water but not gas for a long time, since it was put into production in June 2019, with an average daily water production of 16.53 m³/d and a very clear water quality, representing the communication of the shallow groundwater. In addition, Samples 1 and 3 have lower TDS values than the other produced samples (Table 2) and are determined as dynamic water, which cannot contribute to the reservoir depressurization and gas desorption effectively.

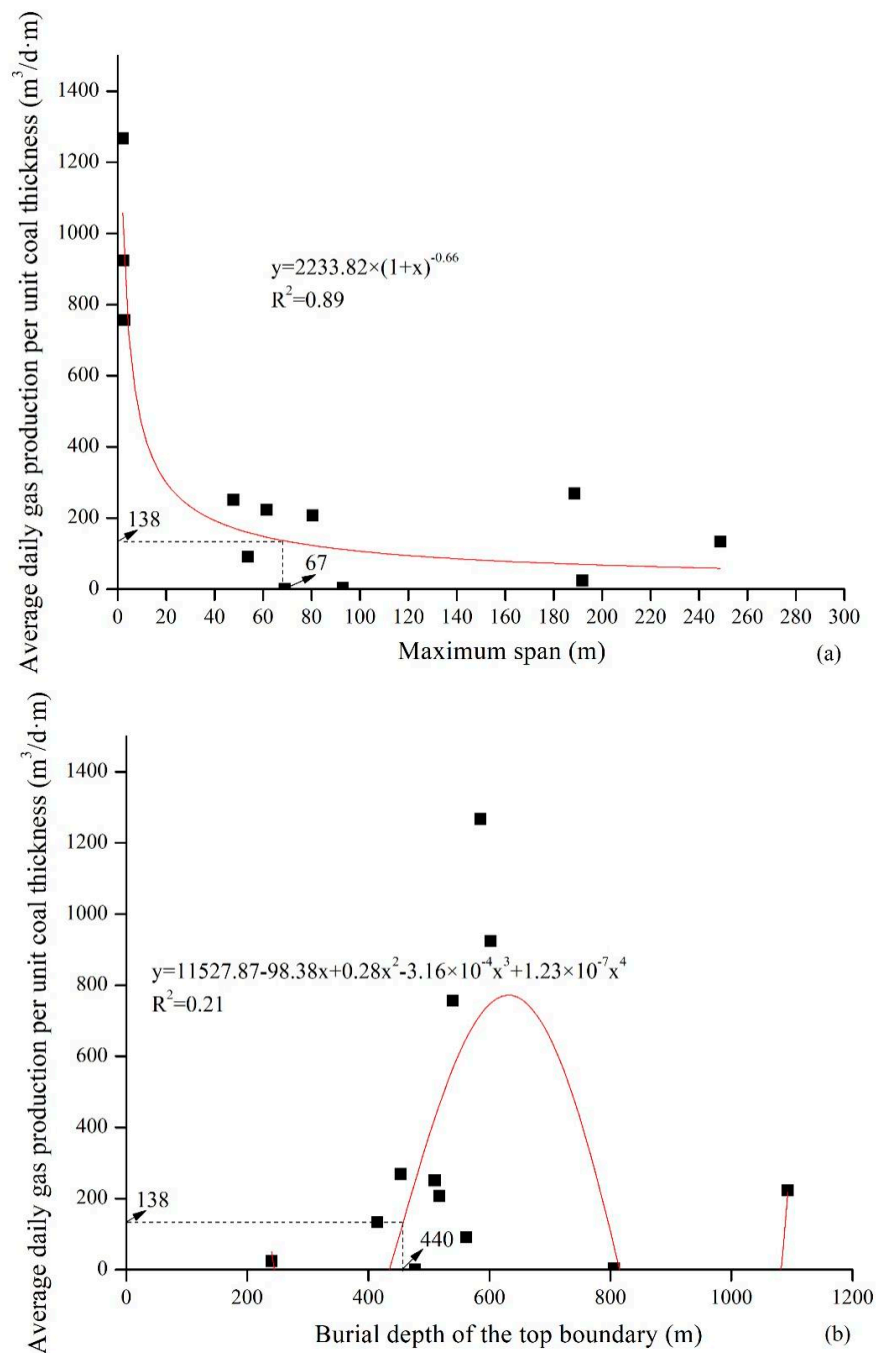


Figure 5. Relationships between the average daily gas production per unit coal thickness and the maximum span (a) and the burial depth of the top boundary of the production coal seam combination (b).

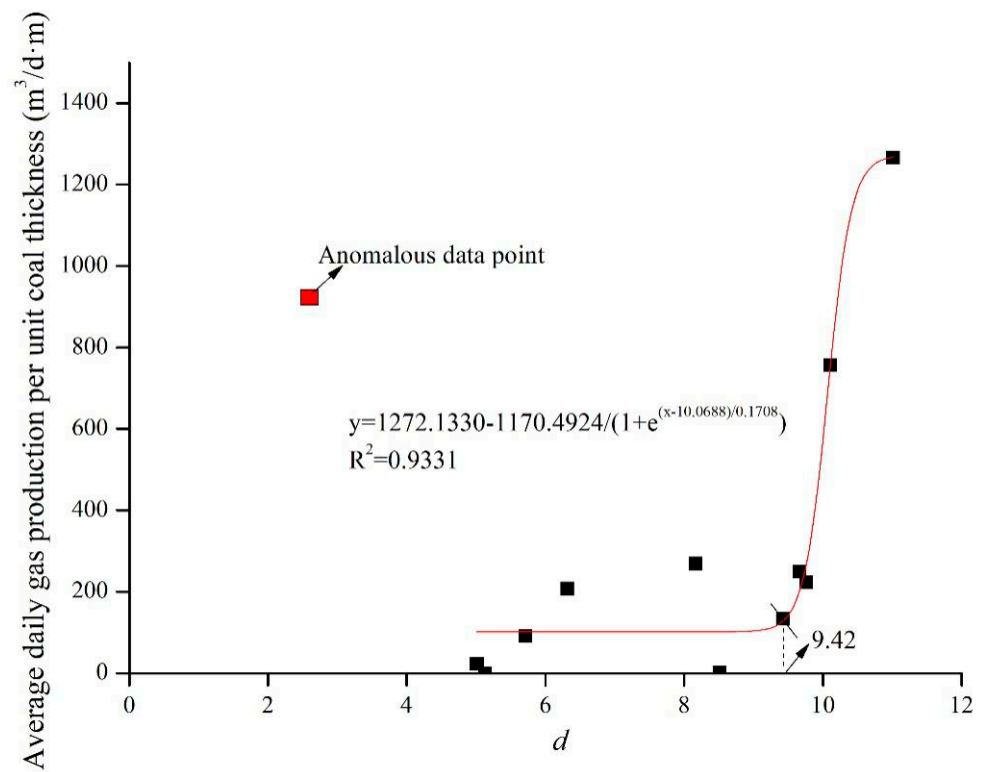


Figure 6. Relationship between d and the average daily gas production per unit coal thickness.

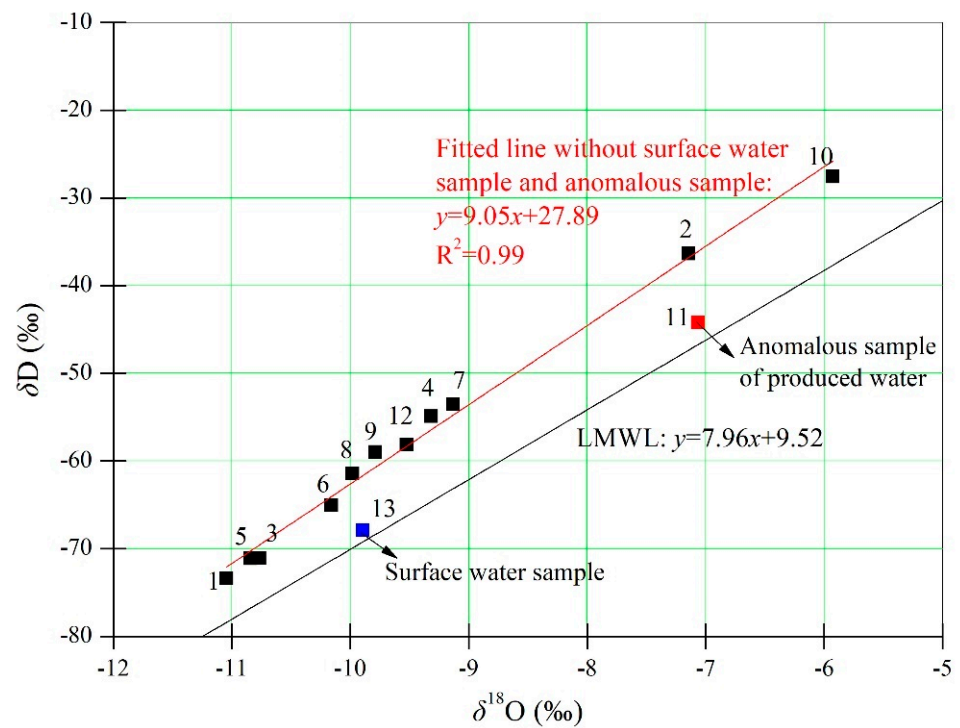


Figure 7. Linear fitting of δD and $\delta^{18}O$ in the produced water samples.

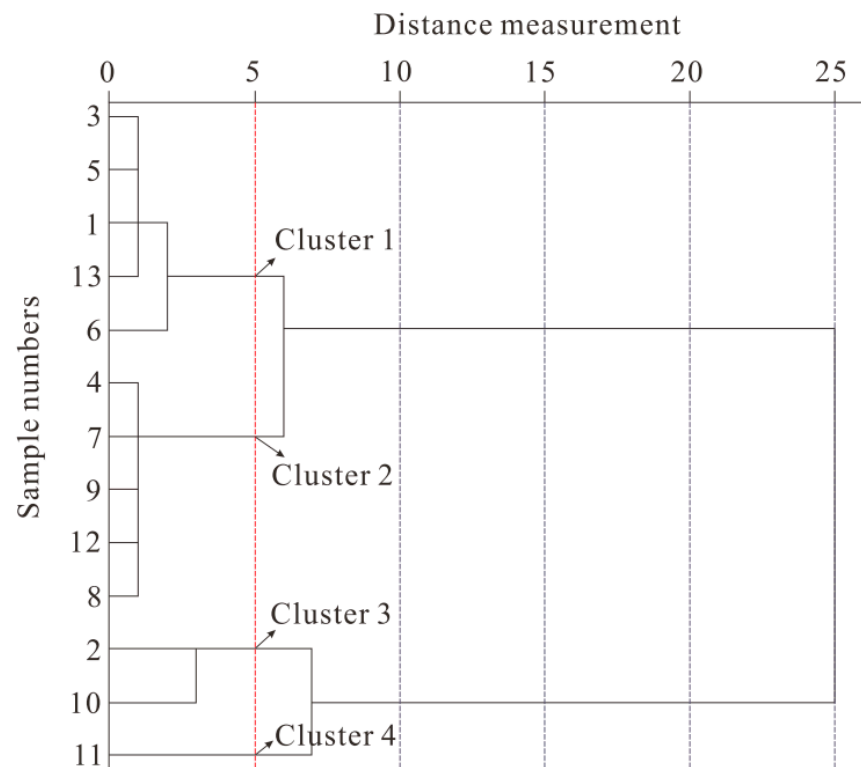


Figure 8. Q-mode cluster analysis of the water samples.

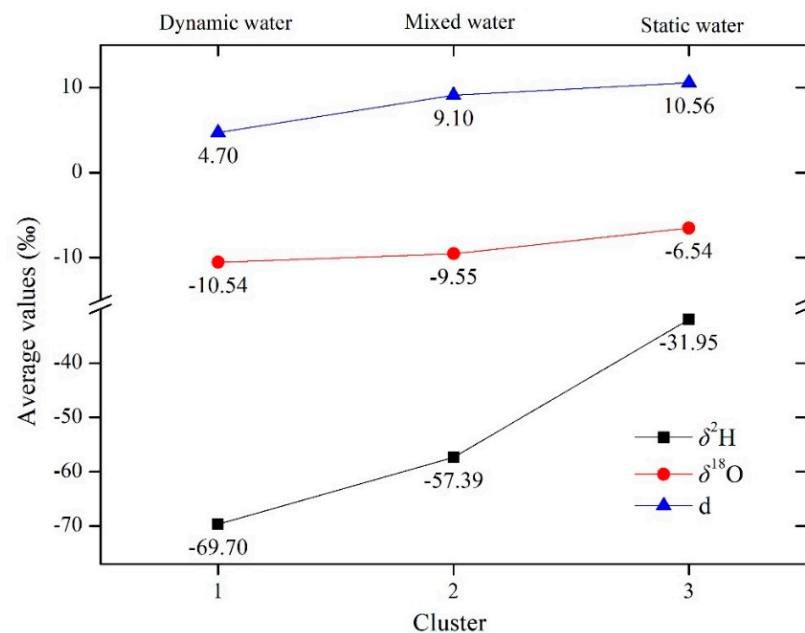


Figure 9. Comparison of the average isotope values of the three clusters.

- (2) The second group (Cluster 2) includes Samples 4, 7, 8, 9, and 12 with heavier hydrogen and oxygen isotopic compositions than those of Cluster 1 (Figures 8 and 9). δD and $\delta^{18}\text{O}$ were -61.41 – -53.52 ‰ (average -57.39 ‰) and -9.98 – -9.13 ‰ (average -9.55 ‰) and the d values were between 8.16 and 9.76 (average 9.10). The wells of this group include three vertical wells and two directional wells and have a higher gas production and lower water production than those of Cluster 1. The average daily gas production per unit coal thickness ranges from 2.54 to 268.89 $\text{m}^3/\text{d}\cdot\text{m}$ (average 175.63 $\text{m}^3/\text{d}\cdot\text{m}$); the average daily water production ranges from 0 to 6.82 m^3/d

- (average $2.07 \text{ m}^3/\text{d}$). Hence, it can be reasonably speculated that this group of water samples represents a mixture of dynamic water and static water.
- (3) The third group (Cluster 3) includes Samples 2 and 10, with relatively heavy hydrogen and oxygen isotopic compositions (Figures 8 and 9). The corresponding well type is horizontal. δD and $\delta^{18}\text{O}$ were from -36.33 to -27.56‰ (average -31.95‰) and -7.14‰ to -5.93‰ (average -6.54‰), respectively. The d values were between 10.11 and 11.02 (average 10.56). The isotopic geochemical characteristics reflect the strong stagnant characteristic of the produced water, corresponding to a high gas production. The average daily gas production per unit coal thickness ranges from 756.43 to $1266.67 \text{ m}^3/\text{d}\cdot\text{m}$ (average $1011.55 \text{ m}^3/\text{d}\cdot\text{m}$); the average daily water production ranges from 0 to $4.24 \text{ m}^3/\text{d}$ (average $2.12 \text{ m}^3/\text{d}$). The horizontal wells are not easy to communicate with the aquifer, and the produced water has low chances of being recharged by an external water source. In addition, the depth of the producing coal seams of Cluster 3 exceeds 500 m , indicating better confinement conditions. This group reflects the static water characteristics of the coal seam and corresponds to a high gas production with an efficient reservoir depressurization.
 - (4) The fourth group (Cluster 4) only includes Sample 11, an anomalous data point, which was consistent with the cluster analysis, and no further detailed analysis was made here.

It can be seen that the isotopic compositions of the produced water are closely related to the level of gas and water production, and the internal reason lies in the difference of the produced water sources. When the water comes from the stagnant static water of the coal seam with a strong water/rock interaction, it is characterized by the heavy hydrogen/oxygen isotopic composition and is conducive to achieving a high gas production efficiency (Cluster 3). Further, when the produced water is recharged by the dynamic water from aquifers or surface water, it is characterized by the light hydrogen/oxygen isotopic composition, corresponding to a low gas production efficiency (Cluster 1) (Figures 9 and 10). In terms of the well type, the vertical well is easy to communicate with the aquifers and easily forms a dynamic water type, resulting in a low gas production efficiency, while the horizontal well easily forms a static water type without communication with the aquifers, resulting in a high gas production efficiency (Figure 10). Therefore, it is important to effectively distinguish the water sources in the produced water and to realize the quantitative separation of dynamic water and static water to identify the degree of interference from the aquifers and predict the gas production efficiency.

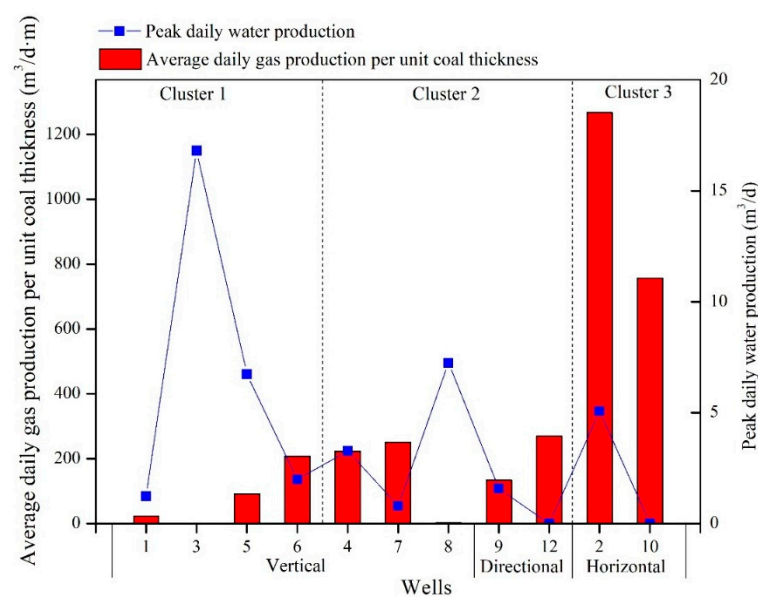


Figure 10. Gas and water production of the CBM wells with the three clusters.

4.4. Quantitative Identification of the Produced Water Sources

According to the results of the cluster analysis, Cluster 1 was regarded as dynamic water in the produced water that recharged from the shallow groundwater (including surface water) and Cluster 3 was regarded as static water within the coal seams. The data of the isotopic compositions for both types of water sources show a linear relationship. Accordingly, the proportions of the static and dynamic water of the samples of Cluster 2 (mixed type) can be quantitatively determined. (1) A linear fit was performed on the data of Clusters 1 and 3 to obtain the fitted linear equation of the dynamic and static waters. (2) The coordinates of the midpoints of the fitted lines are taken as the characteristic values of the stable isotopic compositions of the two water sources: dynamic water and static water. (3) The linear distance between the data point of Cluster 2 and the above two characteristic values of the dynamic and static water was calculated using

$$L = \sqrt{(x_1 - x_2)^2 + (y_1 - y_2)^2} \tag{7}$$

where L is the linear distance between the two points and (x_1, y_1) and (x_2, y_2) are the coordinates of the two points. The closer the distance, the greater the contribution of the corresponding water source. The quantitative contribution of the two water source types can be obtained, based on the relative proportions of the two distances. The calculation formula is

$$P_d = L_s / (L_s + L_d) \tag{8}$$

$$P_s = L_d / (L_s + L_d) \tag{9}$$

where P_d and P_s are the proportions of dynamic water and static water in the water samples, respectively, and L_d and L_s are the distances between the data points of Cluster 2 and the characteristic values of dynamic and static water, respectively. The calculation results are shown in Figure 11.

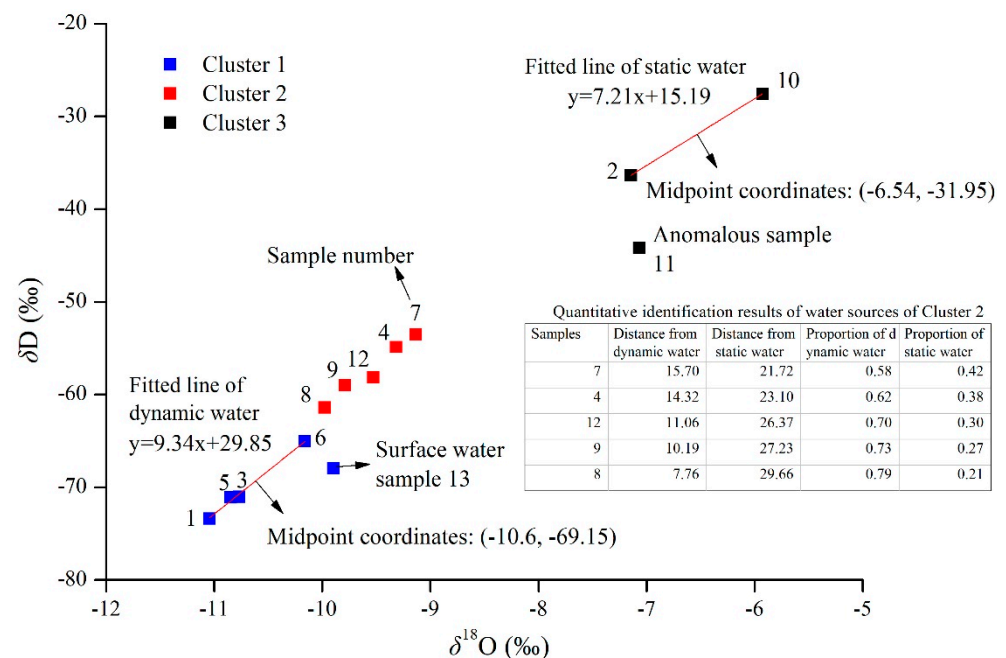


Figure 11. Quantitative identification of the produced water sources between dynamic water and static water.

The proportion of static water in the produced water samples of Cluster 2 does not exceed 0.5, with a maximum value of 0.42 (Sample 7), indicating the dominant dynamic water in the produced water, which in turn inhibits the gas production. This phenomenon is mainly due to the high recharge capacity of dynamic water, which can inhibit the output of

static water. The abundant precipitation and widely developed karst aquifers in the shallow strata in Western Guizhou Province, contribute to the huge amount of dynamic water [7]. Additionally, the water pressure of the upper aquifers is higher than that of the underlying coal seams [47–49], which further promotes the shallow groundwater interference. The cluster analysis also shows the close relationship of Cluster 1 and Cluster 2, which are merged into one cluster with a distance greater than 6 (Figure 8).

The proportion of static water in the produced water samples has a positive correlation with the average daily gas production per unit coal thickness and a negative correlation with the average daily water production (Figure 12). The correlation with gas is better than that with water, indicating that the static water output helps lower the reservoir pressure and improve the gas production efficiency. However, the correlation coefficient was generally not high, due to the variations in the well types. The samples from the two directional wells in Figure 12 are located above the fitted line of the gas production and below the fitted line of the water production, while the samples from the vertical wells are exactly the opposite. This finding reflects the inherent difference in the productivity effect of the well types, with the directional wellbeing more conducive to the gas production than the vertical well [50–54]. In addition, it reflects the reliability of the water source identification made herein after excluding the influence of the well types.

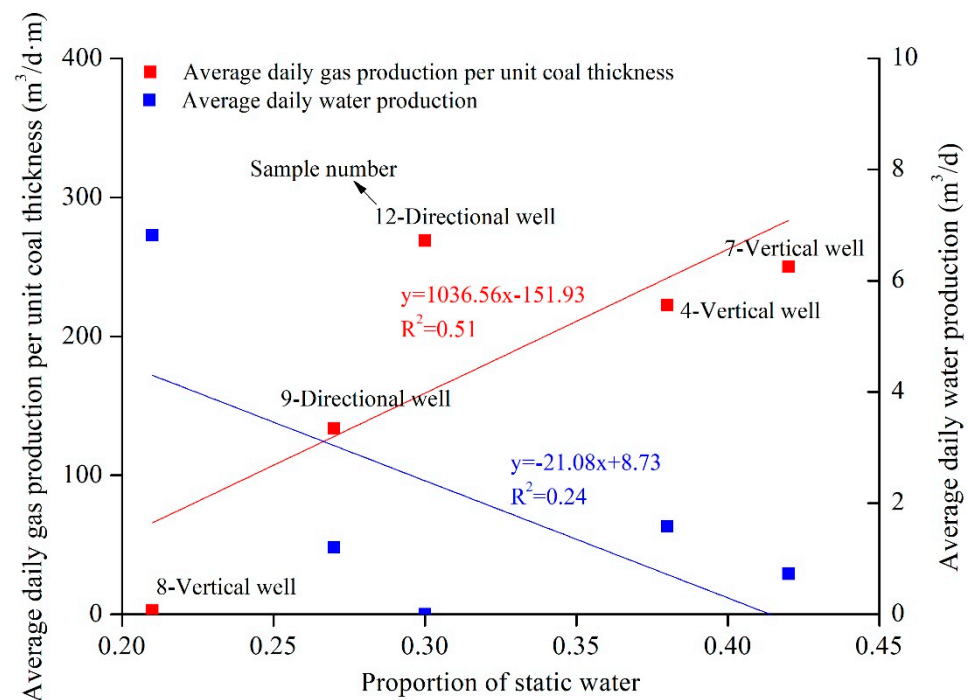


Figure 12. Relationships between the proportion of static water and gas/water production.

5. Conclusions

- (1) The produced water samples in the Zhijin block have δD and $\delta^{18}O$ of -73.37‰ – -27.56‰ (average -56.30‰) and -11.04‰ – -5.93‰ (average -9.23‰), respectively. The surface water samples are close to the LMWL with relatively light isotopic compositions, and the produced water samples are located above and distributed along the LMWL, showing the D-drift characteristics. The differences of the isotopic compositions among the samples form the basis for identifying the sources of produced water;
- (2) d is defined to quantitatively characterize the degree of the D-drift. The larger the span and the shallower the top boundary depth of the production seam combination, the lighter the isotopic compositions and the weaker the D-drift degree of the produced water, representing a higher probability that the produced water is recharged from the upper aquifers;

- (3) The produced water samples are classified into three groups, namely, static water type, dynamic water type, and mixed water type. Based on the determination of the hydrogen and oxygen isotopic eigenvalues of the dynamic water and the static water, the quantitative identification of the water sources of the mixed type and the ratio of the dynamic water and static water in the produced water are conducted. Accordingly, a quantitative identification method for the composition of dynamic and static water sources of the produced water is developed. The results show a clear correlation with the gas and water production of the CBM wells. Producing static water helps promote the reservoir depressurization and improve the gas production efficiency.

Author Contributions: Conceptualization, L.L. and C.G.; methodology, L.L.; software, C.G.; validation, Z.C.; formal analysis, H.Y.; investigation, L.L. and C.G.; resources, H.Y.; data curation, Z.C.; writing—original draft preparation, L.L.; writing—review and editing, C.G.; visualization, Z.C.; supervision, H.Y.; project administration, H.Y.; funding acquisition, C.G. All authors have read and agreed to the published version of the manuscript.

Funding: This work was funded by the National Natural Science Foundation of China (Grant No. 42002195); Guizhou Provincial Science and Technology Program: Qiankehe Strategic Mineral Search [2022] (Grant No. ZD001-01); Open Fund of Key Laboratory of Coalbed Methane Resources and Reservoir Formation Process of the Ministry of Education (China University of Mining and Technology) (Grant No. 2020-002); Outstanding Youth Science Fund of Xi'an University of Science and Technology (Grant No. 2021-14).

Institutional Review Board Statement: Not applicable.

Informed Consent Statement: Not applicable.

Data Availability Statement: Not applicable.

Acknowledgments: We thank all parties and individuals that contributed to this publication.

Conflicts of Interest: The authors declare no conflict of interest.

References

1. Sang, S.X.; Wang, R.; Zhou, X.Z.; Huang, H.Z.; Liu, S.Q.; Han, S.J. Review on carbon neutralization associated with coal geology. *Coal Geol. Explor.* **2021**, *49*, 1–11.
2. Qin, Y.; Shen, J.; Shi, R. Strategic value and strategic choice of China's coal gas industry construction. *J. China Coal Soc.* **2022**, *47*, 371–387.
3. Guo, C.; Gou, J.; Ma, D.M.; Bao, Y.; Shi, Q.M.; Meng, J.H.; Gao, J.Z.; Lu, L.L. Adsorption and desorption behavior under coal-water-gas coupling conditions of high- and low-rank coal samples. *Front. Earth Sci.* **2022**, 1–15. [[CrossRef](#)]
4. Ripepi, N.; Louk, K.; Amante, J.; Schlosser, C.; Tang, X.; Gilliland, E. Determining coalbed methane production and composition from individual stacked coal seams in a multi-zone completed gas well. *Energies* **2017**, *10*, 1533. [[CrossRef](#)]
5. Qin, Y.; Wu, J.; Li, G.; Wang, Y.; Shen, J.; Zhang, B.; Shen, Y. Patterns and pilot project demonstration of coal measures gas production. *J. China Coal Soc.* **2020**, *45*, 2513–2522.
6. Zou, C.N.; Yang, Z.; Huang, S.P.; Ma, F.; Sun, Q.P.; Li, F.H.; Pan, S.Q.; Tian, W.G. Resource types, formation, distribution and prospects of coal-measure gas. *Pet. Explor. Dev.* **2019**, *46*, 451–462. [[CrossRef](#)]
7. Guo, C.; Qin, Y.; Xia, Y.C.; Ma, D.M.; Han, D.; Chen, Y.; Chen, W.; Jian, K.; Lu, L.L. Geochemical characteristics of water produced from CBM wells and implications for commingling CBM production: A case study of the Bide-Santang Basin, western Guizhou, China. *J. Petrol. Sci. Eng.* **2017**, *159*, 666–678. [[CrossRef](#)]
8. Guo, C.; Qin, Y.; Wu, C.F.; Lu, L.L. Hydrogeological control and productivity modes of coalbed methane commingled production in multi-seam areas: A case study of the Bide-Santang Basin, western Guizhou, South China. *J. Petrol. Sci. Eng.* **2020**, *189*, 107039. [[CrossRef](#)]
9. Guo, C.; Qin, Y.; Ma, D.M.; Xia, Y.C.; Bao, Y.; Chen, Y.; Lu, L.L. Pore Structure and Permeability Characterization of High-rank Coal Reservoirs: A Case of the Bide-Santang Basin, Western Guizhou, South China. *Acta Geol. Sin.-Engl. Ed.* **2020**, *94*, 243–252. [[CrossRef](#)]
10. Guo, C.; Qin, Y.; Ma, D.M.; Lu, L.L. Pore structure response of sedimentary cycle in coal-bearing strata and implications for independent superposed coalbed methane systems. *Energy Sources Part A Recovery Util. Environ. Eff.* **2020**, 1–20. [[CrossRef](#)]
11. Guo, C.; Qin, Y.; Sun, X.Y.; Wang, S.M.; Xia, Y.C.; Ma, D.M.; Bian, H.Y.; Shi, Q.M.; Chen, Y.; Bao, Y.; et al. Physical simulation and compatibility evaluation of multi-seam CBM co-production: Implications for the development of stacked CBM systems. *J. Petrol. Sci. Eng.* **2021**, *204*, 108702. [[CrossRef](#)]

12. Guo, T. The enrichment and high yield law of CBM in Yanjiao syncline in Zhijin Block, Guizhou Province. *Coal Geol. Explor.* **2021**, *49*, 62–69.
13. Yang, Z.; Zhang, Z.; Qin, Y.; Wu, C.; Yi, T.; Li, Y.; Tang, J.; Chen, J. Optimization methods of production layer combination for coalbed methane development in multi-coal seams. *Petrol. Explor. Dev.* **2018**, *45*, 312–320. [[CrossRef](#)]
14. Nelson, P.H. Pore-throat sizes in sandstones, tight sandstones, and shales. *AAPG Bull.* **2009**, *93*, 329–340. [[CrossRef](#)]
15. Pashin, J.C. Variable gas saturation in coalbed methane reservoirs of the Black Warrior Basin: Implications for exploration and production. *Int. J. Coal Geol.* **2010**, *82*, 135–146. [[CrossRef](#)]
16. Ryan, D.; Hall, A.; Erriah, L.; Wilson, P. The Walloon coal seam gas play, Surat Basin, Queensland. *APPEA J.* **2012**, *52*, 273–290. [[CrossRef](#)]
17. Zhang, Z.; Qin, Y.; Bai, J.; Li, G.; Zhuang, X.; Wang, X. Hydrogeochemistry characteristics of produced waters from CBM wells in Southern Qinshui Basin and implications for CBM commingled development. *J. Nat. Gas Sci. Eng.* **2018**, *56*, 428–443. [[CrossRef](#)]
18. Liu, G.; Meng, Z.; Luo, D.; Wang, J.; Gu, D.; Yang, D. Experimental evaluation of interlayer interference during commingled production in a tight sandstone gas reservoir with multi-pressure systems. *Fuel* **2020**, *262*, 116557. [[CrossRef](#)]
19. Van Voast, W.A. Geochemical signature of formation waters associated with coalbed methane. *AAPG Bull.* **2003**, *87*, 667–676. [[CrossRef](#)]
20. Rice, C.A. Production waters associated with the Ferron coalbed methane fields, central Utah: Chemical and isotopic composition and volumes. *Int. J. Coal Geol.* **2003**, *56*, 141–169. [[CrossRef](#)]
21. Kinnon, E.C.P.; Golding, S.D.; Boreham, C.J.; Baublys, K.A.; Esterle, J.S. Stable isotope and water quality analysis of coal bed methane production waters and gases from the Bowen Basin, Australia. *Int. J. Coal Geol.* **2010**, *82*, 219–231. [[CrossRef](#)]
22. Golding, S.D.; Boreham, C.J.; Esterle, J.S. Stable isotope geochemistry of coal bed and shale gas and related production waters: A review. *Int. J. Coal Geol.* **2013**, *120*, 24–40. [[CrossRef](#)]
23. Qin, Y.; Moore, T.A.; Shen, J.; Yang, Z.; Shen, Y.; Wang, G. Resources and geology of coalbed methane in China: A review. *Int. Geol. Rev.* **2018**, *60*, 777–812. [[CrossRef](#)]
24. Zhao, Y.; Sun, F.; Wang, B.; Xiong, X.; Li, W.; Cong, L.; Yang, J.; Wang, M. Prediction of Hydrogeological Features and Hydrocarbon Enrichment Zones in Well Area BQ of HanCheng Block, East Ordos Basin, China. In Proceedings of the SPE Annual Technical Conference and Exhibition, Dubai, United Arab Emirates, 26–28 September 2016; pp. 26–28.
25. Brinck, E.L.; Drever, J.E.; Frost, C.D. The geochemical evolution of water coproduced with coalbed natural gas in the Powder River Basin, Wyoming. *Environ. Geosci.* **2008**, *15*, 153–171. [[CrossRef](#)]
26. Cheung, K.; Sanei, H.; Klassen, P.; Mayer, B.; Goodariz, F. Produced fluids and shallow groundwater in coalbed methane (CBM) producing regions of Alberta, Canada: Trace element and rare earth element geochemistry. *Int. J. Coal Geol.* **2009**, *77*, 338–349. [[CrossRef](#)]
27. Dahm, K.G.; Guerra, K.L.; Xu, P.; Drewes, J.E. Composite geochemical database for coalbed methane produced water quality in the rocky mountain region. *Environ. Sci. Technol.* **2011**, *45*, 7655–7663. [[CrossRef](#)]
28. Dahm, K.G.; Guerra, K.L.; Munakata-Marr, J.; Drewes, J.E. Trends in water quality variability for coalbed methane produced water. *J. Clean. Prod.* **2014**, *84*, 840–848. [[CrossRef](#)]
29. Baublys, K.A.; Hamilton, S.K.; Golding, S.D.; Vink, S.; Esterle, J. Microbial controls on the origin and evolution of coal seam gases and production waters of the Walloon Subgroup, Surat Basin, Australia. *Int. J. Coal Geol.* **2015**, *147–148*, 85–104. [[CrossRef](#)]
30. Schofield, S.; Jankowski, J. Hydrochemistry and isotopic composition of NaHCO₃-rich groundwaters from the Ballimore region, central New South Wales, Australia. *Chem. Geol.* **2004**, *211*, 111–134. [[CrossRef](#)]
31. Rice, C.A.; Flores, R.M.; Stricker, G.D.; Ellis, M.S. Chemical and stable isotopic evidence for water/rock interaction and biogenic origin of coalbed methane, Fort Union Formation, Powder River Basin, Wyoming and Montana U.S.A. *Int. J. Coal Geol.* **2008**, *76*, 76–85. [[CrossRef](#)]
32. Sharma, S.; Baggett, J.K. Application of carbon isotopes to detect seepage out of coalbed natural gas produced water impoundments. *Appl. Geochem.* **2011**, *26*, 1423–1432. [[CrossRef](#)]
33. Ma, X.; Song, Y.; Liu, S.; Jiang, L.; Hong, F. Origin and evolution of waters in the Hancheng coal seams, the Ordos Basin, as revealed from water chemistry and isotope (H, O, 129I) analyses. *Sci. China Earth Sci.* **2013**, *56*, 1962–1970. [[CrossRef](#)]
34. Wang, B.; Sun, F.; Tang, D.; Zhan, Y.; Song, Z.; Tao, Y. Hydrological control rule on coalbed methane enrichment and high yield in FZ block of Qinshui Basin. *Fuel* **2015**, *140*, 568–577. [[CrossRef](#)]
35. Wang, S.; Tang, S.; Wan, Y.; Li, Z.; Zhang, S. The hydrogen and oxygen isotope characteristics of drainage water from Taiyuan coal reservoir. *J. China Coal Soc.* **2013**, *38*, 448–454.
36. Zhang, S.; Tang, S.; Li, Z.; Guo, Q.; Pan, Z. Stable isotope characteristics of CBM co-produced water and implications for CBM development: The example of the Shizhuangnan block in the southern Qinshui Basin, China. *J. Nat. Gas Sci. Eng.* **2015**, *27*, 1400–1411. [[CrossRef](#)]
37. Yang, Z.; Wu, C.; Zhang, Z.; Jin, J.; Zhao, L.; Li, Y. Geochemical significance of CBM produced water: A case study of developed test wells in Songhe block of Guizhou province. *J. China Univ. Min. Technol.* **2017**, *46*, 710–717.
38. Qin, Y.; Gao, D.; Wu, C.; Yi, T.; Hong, Y. *Coalbed Methane Resources Potential and Evaluation of Guizhou Province*; China University of Mining and Technology Press: Xuzhou, China, 2012; pp. 12–18.
39. Jin, J.; Tang, X. Structural Features and Their Genesis in Zhijin-Nayong Coalfield, Guizhou Province. *Coal Geol. China* **2010**, *22*, 8–12.

40. Wang, H.; Shao, L.; Hao, L.; Zhang, P.; Glasspool, I.J.; Wheeley, J.R.; Wignall, P.B.; Yi, T.; Zhang, M.; Hilton, J. Sedimentology and sequence stratigraphy of the Lopingian (Late Permian) coal measures in southwestern China. *Int. J. Coal Geol.* **2011**, *85*, 168–183. [[CrossRef](#)]
41. Shen, Y.; Qin, Y.; Wang, G.G.; Guo, Y.; Shen, J.; Gu, J.; Xiao, Q.; Zhang, T.; Zhang, C.; Tong, G. Sedimentary control on the formation of a multi-superimposed gas system in the development of key layers in the sequence framework. *Mar. Pet. Geol.* **2017**, *88*, 268–281. [[CrossRef](#)]
42. Fu, H.J.; Yan, D.T.; Yang, S.G.; Wang, X.M.; Wang, G.; Zhuang, X.G.; Zhuang, L.Y.; Li, G.Q.; Chen, X.; Pan, Z.J. A study of the gas-water characteristics and their implications of the coalbed methane accumulation modes in the Southern Junggar Basin, China. *AAPG Bull.* **2021**, *105*, 189–221. [[CrossRef](#)]
43. Zhu, X.; Liang, J.; Liu, Y.; Wang, C.; Liao, X.; Guo, G.; Lv, Y. Influencing factor and type of water production of CBM wells: Case study of Shizhuangnan block of Qinshui Basin. *Nat. Gas Geosci.* **2017**, *28*, 755–760.
44. Guo, C.; Gao, J.Z.; Wang, S.Q.; Zhang, C.; Li, X.; Gou, J.; Lu, L.L. Groundwater geochemical variation and controls in coal seams and overlying strata in the Shennan mining area, Shaanxi, China. *Mine Water Environ.* **2022**, *41*, 614–628. [[CrossRef](#)]
45. Guo, C.; Qin, Y.; Yi, T.S.; Chen, Z.L.; Yuan, H.; Gao, J.Z.; Gou, J. A method for identifying coalbed methane co-production interference based on production characteristic curves: A case study of the Zhijin block, western Guizhou, China. *Petrol. Explor. Develop.* **2022**, *49*, 1126–1137. [[CrossRef](#)]
46. Guo, C.; Qin, Y.; Yi, T.S.; Ma, D.M.; Wang, S.Q.; Shi, Q.M.; Bao, Y.; Chen, Y.; Qiao, J.W.; Lu, L.L. Review of the progress of geological research on coalbed methane co-production. *Coal Geol. Explor.* **2022**, *50*, 42–57.
47. Guo, C.; Qin, Y.; Ma, D.; Yang, Z.; Lu, L. Prediction of geotemperatures in coal-bearing strata and implications for coal bed methane accumulation in the Bide-Santang basin, western Guizhou, China. *Int. J. Min. Sci. Technol.* **2020**, *30*, 235–242. [[CrossRef](#)]
48. Guo, C.; Qin, Y.; Lu, L. Terrestrial heat flow and geothermal field characteristics in the Bide-Santang basin, western Guizhou, South China. *Energy Explor. Exploit.* **2018**, *36*, 1114–1135. [[CrossRef](#)]
49. Guo, C.; Qin, Y.; Han, D. Interlayer interference analysis based on trace elements in water produced from coalbed methane wells: A case study of the Upper Permian coal-bearing strata, Bide—Santang Basin, western Guizhou, China. *Arab. J. Geosci.* **2017**, *10*, 137. [[CrossRef](#)]
50. Guo, C.; Xia, Y.; Ma, D.; Sun, X.; Dai, G.; Shen, J.; Chen, Y.; Lu, L. Geological conditions of coalbed methane accumulation in the Hancheng area, southeastern Ordos Basin, China: Implications for coalbed methane high-yield potential. *Energy Explor. Exploit.* **2019**, *37*, 922–944. [[CrossRef](#)]
51. Guo, C.; Qin, Y.; Ma, D.; Xia, Y.; Chen, Y.; Si, Q.; Lu, L. Ionic composition, geological signature and environmental impacts of coalbed methane produced water in China. *Energy Sources Part A Recovery Util. Environ. Eff.* **2021**, *43*, 1259–1273. [[CrossRef](#)]
52. Wu, J.; Guo, C.; Sang, S.X.; Li, G.F. Geochemical characteristics of water produced from coalbed methane wells in the southern Qinshui Basin and construction of an associated Model: Implications for coalbed methane co-production. *Energies* **2022**, *15*, 8009. [[CrossRef](#)]
53. Mendhe, V.A.; Mishra, S.; Varma, A.K.; Singh, A.P. Coalbed methane-produced water quality and its management options in Raniganj Basin, West Bengal, India. *Appl. Water Sci.* **2017**, *7*, 1359–1367. [[CrossRef](#)]
54. Shi, Q.M.; Cui, S.D.; Wang, S.M.; Mi, Y.C.; Sun, Q.; Wang, S.Q.; Shi, C.Y.; Yu, J.Z. Experiment study on CO₂ adsorption performance of thermal treated coal: Inspiration for CO₂ storage after underground coal thermal treatment. *Energy* **2022**, *254*, 124392. [[CrossRef](#)]